Translational Oncology
www.transonc.com

Volume 4 Number 6 December 2011 pp. 365–376 365

Tumor-Endothelial Cell Three-dimensional Spheroids: New Aspects to Enhance Radiation and Drug Therapeutics[1,2]

Meenakshi Upreti*, Azemat Jamshidi-Parsian*, Nathan A. Koonce*, Jessica S. Webber*, Sunil K. Sharma*, Alexzander A.A. Asea†, Mathew J. Mader* and Robert J. Griffin*

*Department of Radiation Oncology, University of Arkansas for Medical Sciences, Little Rock, AR, USA; †Department of Pathology, Scott & White Memorial Hospital and Clinic and Texas A&M Health Science Center, College of Medicine, Temple, TX, USA

Abstract

Classic cancer research for several decades has focused on understanding the biology of tumor cells *in vitro*. However, extending these findings to *in vivo* settings has been impeded owing to limited insights on the impact of microenvironment on tumor cells. We hypothesized that tumor cell biology and treatment response would be more informative when done in the presence of stromal components, like endothelial cells, which exist in the tumor microenvironment. To that end, we have developed a system to grow three-dimensional cultures of GFP-4T1 mouse mammary tumor and 2H11 murine endothelial cells in hanging drops of medium *in vitro*. The presence of 2H11 endothelial cells in these three-dimensional cocultures was found to sensitize 4T1-GFP tumor cells to chemotherapy (Taxol) and, at the same time, protect cells from ionizing radiation. These spheroidal cultures can also be implanted into the dorsal skinfold window chamber of mice for fluorescence imaging of vascularization and disease progression/treatment response. We observed rapid neovascularization of the tumor-endothelial spheroids in comparison to tumor spheroids grown in nude mice. Molecular analysis revealed pronounced up-regulation of several proangiogenic factors in the tumor tissue derived from the tumor-endothelial spheroids compared with tumor-only spheroids. Furthermore, the rate of tumor growth from tumor-endothelial spheroids in mice was faster than the tumor cell–only spheroids, resulting in greater metastasis to the lung. This three-dimensional coculture model presents an improved way to investigate more pertinent aspects of the therapeutic potential for radiation and/or chemotherapy alone and in combination with antiangiogenic agents.

Translational Oncology (2011) 4, 365–376

Introduction

Development of malignancy and response of tumors to therapy depends on their ability to adapt to different environments, compete with normal cells for space and nutrients, and ignore molecular signals that inhibit cell proliferation and promote cell death [1]. The process of initiation and development of the tumor involves (i) the assembly of the proliferating tumor cells into a three-dimensional structure termed *tumorigenesis* and (ii) a complex interaction between tumor cells and their microenvironment termed *tumor angiogenesis* where host endothelial cells (and various other types of cells) are recruited to contribute to the formation of tumor vasculature to

Address all correspondence to: Meenakshi Upreti, PhD, 4301 W Markham St, Little Rock, AR 72205. E-mail: mupreti@uams.edu

[1]The authors thank the research support from the Central Arkansas Radiation Therapy Institute (to M.U./R.J.G.) and the National Cancer Institute (grants CA44114 and CA107160 to R.J.G.). The use of the facilities in the University of Arkansas for Medical Sciences Digital and Confocal Microscopy Laboratory was supported by the National Institutes of Health (grants P20RR16460, S10RR1939, and UL1RR029884), and Dr Richard Kurten's guidance is acknowledged.

[2]This article refers to supplementary material, which is designated by Figure W1 and is available online at www.transonc.com.

Received 24 May 2011; Revised 4 August 2011; Accepted 16 August 2011

DOI 10.1593/tlo.11187

provide an adequate supply of oxygen and nutrients for the growing tumor mass.

Existing preclinical tumor cell *in vitro* models have not explicitly incorporated angiogenesis and thus have ignored the interaction between tumor and endothelial cells *in vitro*. In addition, studies on *in vitro* two-dimensional monolayer cell cultures and their translation/extension to clinical settings have their limitations because they are not capable of mimicking the nutrient and oxygen gradient and an environment reminiscent of the *in vivo* setting [2–4]. Furthermore, obtaining fresh tumor samples in clinical settings can be especially challenging and provides limited possibilities for manipulation. Clinical samples have also been shown to exhibit considerable heterogeneity for a wide variety of reasons [5,6]. Although the rationale behind the use of antiangiogenic and antivascular therapy is solid, a major factor in the somewhat disappointing and even surprising results of the first tumor vasculature–targeted agent human clinical trials may be owing to limitations in the *in vitro* and *in vivo* animal models used to date [7,8]. Therefore, a preclinical *in vitro* model that can facilitate the intra/intercellular crosstalk mimicking the *in vivo* tumor and endothelial cell architecture and, more importantly, lend itself for controlled experimental manipulation and replication would be extremely valuable for interrogating these interactions between tumor parenchyma and stroma to better understand the mechanisms of radiation and cancer therapeutics and promote the establishment of improved pharmacokinetics, efficacy, and safety profiles.

Techniques that allow a coculture of tumor and stromal cells to promote a realistic self assembly into three-dimensional spheroids have been rarely studied to any great detail thus far in the literature. An attempt in this direction was made by Timmins et al. [9] to generate three-dimensional tumor-endothelial spheroids in hanging drops of medium. However, this approach has not evolved beyond its nascent stage, possibly because of the lack of discovery and validation at a molecular level of important signaling mechanisms involved in tumor angiogenesis and the fact that the spheroids were not transplanted into animal models for studying cancer progression and ultimately metastasis. We have recently discovered that certain pairs of endothelial and tumor cell lines grow exceedingly well together in a hanging drop, compared with either cell type alone. In the current study, we have used the GFP-4T1 mouse mammary tumor cells and 2H11 murine endothelial cells as a three-dimensional coculture model for studying the effects of treatment on tumor angiogenesis and tumor cell survival and have monitored tumor growth and metastatic activity by implanting these tumor-endothelial spheroids in the dorsal skinfold window chamber or rear limb of immunocompromised mice. Using this system to coculture tumor and endothelial cells in three dimensions, we have monitored response to chemotherapy or radiotherapy *in vitro* and in the development of vessels and tumor growth and metastasis *in vivo*. This *in vitro*/*in vivo* tumor-endothelial coculture is, to our knowledge, the first preclinical model that is able to provide an understanding of cancer in a continuum—from initiation to development and progression. Our primary goal was to use this system to understand more accurately the mechanisms by which primary or metastatic tumor tissue grows and responds to novel angiogenesis-targeted treatments and radiation therapy. We surmise that this *in vitro*/*in vivo* preclinical mouse model will not only enable the identification of authentic and novel biomarkers but also provide enhanced predictive utility for drug development and discovery.

Materials and Methods

Cell Lines and Culture

GFP-4T1 [10] is a green fluorescent protein (GFP)–expressing mouse metastatic mammary epithelial cell line that is resistant to Taxol [11]. The 2H11 cell line was validated as a tumor-like endothelial cell line by Walter-Yohrling et al. [12]. Most endothelial cell lines being used to study angiogenesis have been immortalized using SV40 and express the SV40 T antigen, with the assumption that SV40 is nonpermissive in murine cells. Although transformed, these cell lines tend to retain most of the normal cellular physiology and functional characteristics of endothelial cells. 2H11 is one such endothelial cell line originally generated by O'Connell and Rudmann [13], O'Connell and Edidin [14], and O'Connell et al. [15] from endothelial cells isolated from lymph nodes of adult C3H/HeJ mice transformed using SV40 displaying characteristics of Kaposi sarcoma. This cell line is most well characterized by the presence of several attributes typical of normal endothelial cells and those of endothelial cells directly isolated from tumors. Walter-Yohrling et al. [12] thus termed this cell type as *tumor-endothelial cells*. The standard endothelial cell markers found in this cell type, some of which we have also verified in this article, include sialomucin/CD34, GPIIIB/CD36, endogolin/CD105, P1H12/CD146, VCAM1/106, Tie-1, and Tie-2. The tumor-endothelial markers that are expressed in relatively high levels include mTEM1, mTEM5, mTEM7, and mTEM8. This murine endothelial cell line also responds to antiangiogenic agents by inhibition of proliferation and tube formation. It has been identified as a murine endothelial cell line to model tumor endothelium for studying the antiangiogenic activity of therapeutic compounds *in vitro* and is therefore our choice for representing the endothelial component in our model. The cell lines were maintained as monolayer culture at 37°C and 5% CO_2 in Dulbecco modified Eagle medium (Mediatech, Manassas, VA), supplemented with 10% fetal bovine serum (Atlas, Fort Collins, CO), 100 U/ml penicillin, and 100 μg/ml streptomycin (HyClone, South Logan, UT).

Chemicals and Reagents

Paclitaxel (Taxol), dimethyl sulfoxide (DMSO), and MitoTracker Red CMXRos were purchased from Sigma-Aldrich, Inc (St Louis, MO), Research Organics (Cleveland, OH), and Invitrogen (Carlsbad, CA) respectively. Antibodies to murine NOV/CCN3, murine interleukin 1α, and rat matrix metalloproteinase 8 (MMP-8) for reverse-phase immunoblot analysis were obtained from R&D Systems (Minneapolis, MN). The glyceraldehyde-3-phosphate dehydrogenase antibody was from Cell Signaling Technology (Danvers, MA). The MMP-9 antibody was obtained from Abcam (Cambridge, MA). The antibodies galectin-1 (Santa Cruz Biotechnology, Santa Cruz, CA), CD34 (BD Pharmingen, Sparks, MD), and human von Willebrand factor (vWF; Dako Denmark A/S, Glostrup, Denmark) were used for immunoblot analysis and immunostaining to identify the tumor-endothelial cells in spheroids.

Spheroid Culture in "Hanging Drop"

GFP-4T1 tumor cells and 2H11 endothelial cells were used to generate multicellular spheroids by growing them as "hanging drops" of medium (in Dulbecco modified Eagle medium with 10% fetal bovine serum and antibiotic/antimycotic mix) [16]. Briefly, single-cell suspension of GFP-4T1 cells (1000 cells/20 μl) was dispensed on the inside of the lid of each well of a 48-well cell culture plate (Greiner

Cellstar, BioExpress, Kaysville, UT). Gravity-enforced self-aggregation of cells was facilitated by inverting the lid and setting it on the plate and incubating under standard conditions. At day 3, the lids were set upright, and 2000 cells in a volume of 5 μl, 2H11 endothelial, or additional GFP-4T1 tumor cells were introduced to the existing culture. These cultures were reinverted and left as hanging drops and incubated further for 10 to 14 days. The day tumor or endothelial cells were reintroduced to the tumor cell aggregates in the hanging drop of medium was taken as day 1 in all experiments. Introduction of 1/10th the number of tumor or endothelial cells to the existing hanging drop culture of 4T1 tumor cells did not change the pattern of growth and morphology of the spheroids (Figure W1). Because the proliferation of cells in spheroids is not as fast as that observed in monolayer cell cultures and to generate adequate numbers of each cell type from the spheroids to assess the treatment response when tumor and endothelial cells were in contact, we opted to do our experiments using spheroids prepared by the introduction of 2000 cells to the existing culture (1:1 ratio). The three-dimensional spheroids composed of GFP-4T1 cells alone are referred to as *tumor cell–only spheroids* and those formed by the coculture of 4T1 and 2H11 cells types are referred to as *tumor-endothelial cell spheroids* in the rest of this report. Both tumor cell–only and tumor-endothelial cell spheroids remain intact and viable at day 10, and therefore, all *in vitro* and *in vivo* experiments have been done using spheroids at day 10 of culture in hanging drops.

Immunohistochemistry

Spheroids were harvested and frozen in OCT (Tissue-Tek, Sakura Finetek USA, Inc, Torrance, CA). A total of 6 to 10 spheroids were embedded in each OCT block. Five- micrometer cryostat sections were immunohistochemically analyzed using standard protocols. The primary antibodies used recognized CD34 at a dilution of 1:50 or vWF at a dilution of 1:200. Fluorescent visualization was performed with 1:200 Northern Lights antirat IG-NL557 (R&D Systems) and 1:200 Cy 3 (Jackson ImmunoResearch Laboratories, Inc, West Grove, PA) antibody, respectively, and counterstained with Vectashield Mounting Medium with 4′,6-diamidino-2-phenylindole (Vector, Burlingame, CA). Slides were observed at 10×, 20×, or 40× using Olympus IX71 microscope and images taken by an Olympus DP72 camera (Olympus, Tokyo, Japan).

Hematoxylin and Eosin Staining and Imaging

Hematoxylin and eosin (H&E) staining was performed by staining the cryostat sections with Harris hematoxylin (aluminum potassium sulfate, hematoxylin, absolute alcohol, mercuric oxide, and glacial acetic acid) followed by 1% acid alcohol and, subsequently, 1% eosin. Images of spheroids were taken at 10× using Olympus IX71 microscope and Olympus DP72 camera. Tissue imaging was performed using an Aperio ScanScope (Aperio, Vista, CA) at 20× magnifications and analyzed using ImageScope software (Aperio).

Stabilization of Spheroids and Confocal Microscopy

Tumor-endothelial cell spheroids consisting of the GFP-4T1 murine mammary epithelial cancer cells stably expressing GFP and the 2H11 murine tumor-endothelial cells and the tumor cell–only (GFP-4T1) spheroids were incubated with 1 μM of MitoSOX Red (Invitrogen) at 37°C for 10 minutes followed by washing twice with phosphate-buffered saline (PBS). The spheroids were then fixed for 3 hours at 4°C in 1% parafomaldehyde (EUROMEDEX, Mundolsheim, France) and washed twice with PBS. SeaPlaque low-melt agarose (0.8%; FMC BioProducts, Rockland, ME) was prepared for use as described by the manufacturer, cooled on ice, and made isotonic by the addition of 40× PBS. SeaPlaque low-melt agarose was added to the spheroids, and then they were loaded onto cooled slides. Double-sided tape was used between the slide and coverslipped to maintain the shape of the tumor spheroids. Imaging was performed using a confocal laser scanning system (LSM 510; Carl Zeiss, Peabody, MA).

Cell Death Assay

At day 10, the spheroids were transferred to a low-binding 96-well plate (Nalgene, Nunc, Japan) and subjected to treatment with drug for 48 hours. After drug treatment, spheroids were dissociated using trypsin. The three-dimensional spheroids developed an extracellular matrix, making it extremely difficult to dissociate the cells; we therefore passed the cells after dissociation through a 40-μm filter to avoid the presence of cell clusters. The suspension is diluted to a concentration of 5×10^4/ml for measurement of apoptosis using a cell death detection ELISA kit (Roche, Indianapolis, IN). This is a quantitative photometric immunoassay for the determination of cytoplasmic histone-associated oligosomes generated during apoptosis. After dilution, cells were centrifuged at 200*g* for 5 minutes, and the cell pellet was resuspended in 0.5 ml of incubation buffer and incubated at room temperature for 30 minutes. After centrifugation at 16,000*g* for 10 minutes, 0.4 ml of supernatant was removed and diluted 1:10 in incubation buffer for analysis. The ELISA plate was prepared according to the manufacturer's instructions, and 0.1 ml of sample was added to the appropriate wells and incubated at room temperature for 90 minutes. After conjugation and incubation with substrate solution, the plate was shaken on an orbital shaker at 250 rpm for 15 minutes, and the absorbance at 405 nm was determined using an ELx800 microplate reader (BioTek, Winooski, VT).

Fluorescence Assay

The tumor cell–only and the tumor-endothelial cell spheroids were transferred to low binding 96-well plates at day 10, and emission of fluorescence was read at 510 nm using a Synergy 2 Multi-Mode Microplate Reader (BioTek). The spheroids were subjected to treatment with Taxol for 48 hours after which the fluorescence intensity was read again. The relative decrease in fluorescence was calculated to assess the response of 4T1 tumor cells to Taxol in the presence of 2H11 endothelial cells.

Survival Assay

The tumor cell–only and tumor-endothelial cell spheroids were transferred to low-binding 96-well plates and irradiated at 2 Gy. Spheroids of each type were pooled and trypsinized, cell clusters were removed by passing through a 40-μm filter, and 200 to 8000 cells of each treatment were plated in triplicate onto a six-well culture dish. Phase-contrast and fluorescence images were taken 2 weeks after plating. A final cell count after 2 weeks for each set was done to estimate the overall survival.

Animals

Female, athymic, nude mice (8-9 weeks old, 20-22 g) were purchased from Charles River Laboratories (Wilmington, MA) and housed in the animal care facility of the University of Arkansas for Medical Sciences. All experiments were carried out in accordance with protocols approved

by the Institutional Animal Care and Use Committee at the University of Arkansas for Medical Sciences. The mice were given clean water *ad libitum* and 2016 Teklad Global 16% Protein Rodent Diet (Harlan Feeds, Woodland, CA).

Animal Model and Surgical Techniques

All surgical procedures were performed in a sterile field. Dorsal skin window chambers and surgical instruments were autoclaved before use. Saline used to keep tissue moist during surgical preparation was mixed with gentamicin (50 μl/ml).

Dorsal skinfold window chamber model. The dorsal skin window chamber in the mouse was prepared as described [17,18]. Briefly, female mice (20-22 g body weight) were anesthetized (inhalant isoflurane at 3% maintenance) and placed on a heating pad. Two symmetrical titanium frames were implanted into a dorsal skinfold, to sandwich the extended double layer of skin. An approximately 15 × 15-mm^2 layer was excised. Two three-dimensional spheroids of each type at day 10 after coculture in hanging drops of medium were placed on the underlying cutaneous maximus muscle and subcutaneous tissues of each mouse, which were subsequently covered with a glass coverslip incorporated in one of the frames. After a recovery period of 1 to 2 days, the windows were imaged for neovascularization using an Olympus IX71 microscope and an Olympus DP72 camera.

Blood Vessel Extraction Using MATLAB

Using a computer program created in house, two-dimensionally projected vascular networks were produced from the region of interest selected from images recorded with the 4× objective. The algorithms used for identification of the vascular networks were implemented by use of the MATLAB software (MathWorks, Natick, MA). The extraction technique involved a series of filtering, threshold, and other morphologic image analysis procedures to get vascular tree structure. Finally, binary images of blood vessel structure were assigned the intensity of the input image [19].

Rear limb model. A small incision was made in the right hind limb above the ankle and two three-dimensional spheroids at day 10 after coculture in hanging drops of medium were implanted in the exposed subcutaneous tissue of each mouse. The incision was then sutured with tissue adhesive (3M VetBond, St Paul, MN). Tumor growth was recorded by caliper measurement. The mean of two perpendicular diameters was obtained. Tumor diameters were measured

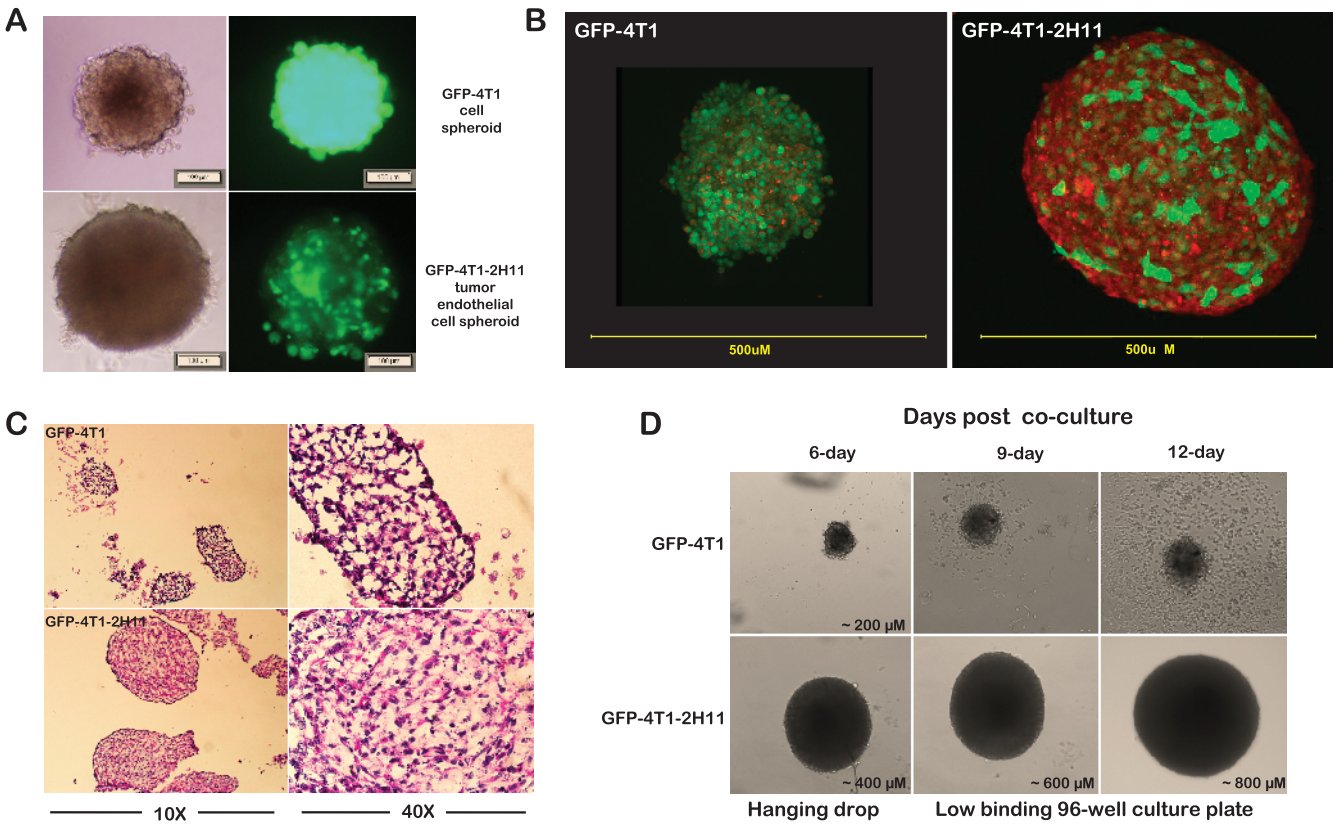

Figure 1. Hanging drop cultures of three-dimensional spheroids. (A) Bright field and fluorescence images of GFP-4T1 mouse mammary metastatic carcinoma cells alone (tumor cell only; upper panel) and grown in association with 2H11 murine endothelial cells (tumor-endothelial cells; lower panel) as three-dimensional spheroids in hanging drop cultures for 7 days. Bar, 100 μm. (B) Confocal microscopy of tumor cell–only (GFP-4T1) and tumor-endothelial cell (GFP-4T1–2H11) spheroids at day 7 after coculture after labeling with live cell-permeant MitoTracker Red that stains the mitochondria. The regions where the red and green do not colocalize in the tumor-endothelial spheroid overlay indicate the presence of 2H11 endothelial cells. Images are an overlay of green fluorescence (green) and MitoTracker Red (red). (C) H&E staining of cryostat sections of spheroids at 10× and 40×, 10 days after coculture. (D) Growth of GFP-4T1 and GFP-4T1–2H11 spheroids in hanging drops followed by transfer to low-binding 96-well plates at 6, 9, and 12 days after coculture.

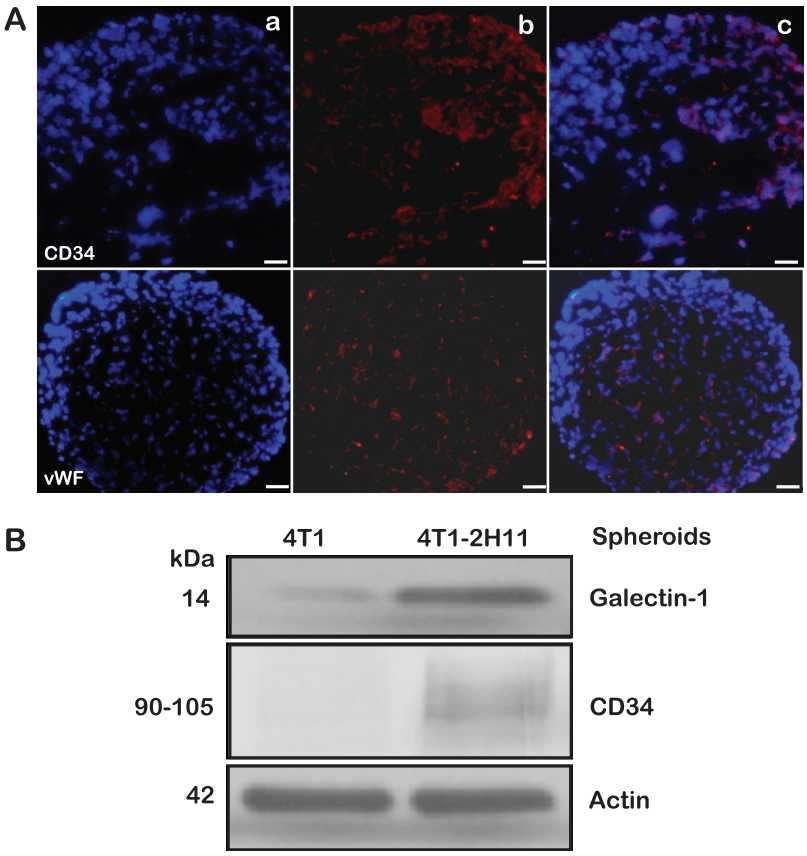

Figure 2. Molecular identification of the endothelial component in the tumor-endothelial cell spheroids. (A) Five-micrometer cryosections of GFP-4T1–2H11 spheroids were analyzed by immunofluorescence at 20× with primary antibodies for CD34 (a marker for tumor-endothelial cells [upper panel]) and vWF that recognizes endothelial cells (lower panel) with Texas Red–labeled secondary antibody for detection. Left to right: (a) DAPI, (b) immunofluorescent signal alone, and (c) overlay. (B) Lysates from GFP-4T1 and GFP-4T1–2H11 spheroids 10 days after coculture were probed for expression Galectin-1 and CD34 by Western immunoblot analysis for the presence of tumor-endothelial–specific cells.

each day. The animals were killed at the end of 33 days. Lung and spleen were excised to observe green fluorescence (GFP-4T1) indicative of possible metastasis.

Intravital Fluorescence Microscopy

The dorsal skinfold window chamber model allows for intravital imaging of the tumor growth and neovascularization. Because the 4T1 tumor cells were GFP positive, the normal and tumor tissue could be easily differentiated. Fluorescence microscopy was performed using an Olympus IX71 microscope, and digital images were taken every 4 days after the window chambers were implanted using an Olympus DP72 camera.

Mouse Angiogenesis Antibody Array

The mice were killed on day 16 after implantation. Tumors originating from tumor cell–only and tumor-endothelial cell three-dimensional spheroids were excised and homogenized in 400 μl of lysis buffer (25 mM HEPES, pH 7.5, 0.5% sodium deoxycholate, 5 mM EDTA, 5 mM dithiothreitol, 20 mM glycerophosphate, 1 mM Na_3VO_4, 50 mM NaF, 1% Triton X-100, 20 μg/ml aprotinin, 50 μg/ml leupeptin, 10 μM pepstatin, 1 μM okadaic acid, and 1 mM phenylmethylsulfonyl fluoride). The lysates were incubated at 4°C and passed through a 21-gauge syringe 10 times, and the insoluble material was removed by centrifugation (15 minutes at 12,000*g*). The protein concentration was determined using the Bio-Rad protein assay. Two hundred micrograms of lysate was hybridized to a mouse angiogenesis antibody array (R&D Systems) as instructed.

Pathway Analysis

The Ingenuity Pathway Analysis Tool was used to generate significant gene networks and examine the functional associations between differentially expressed proteins in the angiogenesis arrays obtained from incubation with lysates of tumors originating from GFP-4T1 tumor and GFP-4T1–2H11 tumor-endothelial spheroids (www.ingenuity.com).

Immunoblot Analysis

Lysates from the three-dimensional spheroid of each type were prepared in the lysis buffer as described. About 10 to 20 spheroids were incubated in the lysis buffer described above at 4°C for 1 hour on NUTATOR (Benchmark Scientific, Inc, Edison, NJ). Cell debris was removed by centrifugation (15 minutes at 12,000*g*). Immunoblot analysis was performed using 50 μg of protein/lane and standard polyvinylidene fluoride membrane transfer followed by probing with the respective antibody and chemiluminescent detection of the bands.

Statistical Analysis

Data are expressed as mean ± 1 SD of at least three different experiments unless otherwise mentioned. Statistical significance of difference in means was performed using the parametric two-sample *t* test with unequal variance (MathWorks). The corresponding *P* values are shown for each of the comparisons under the respective sections.

Results

Tumor Cell–Only Versus *Tumor-Endothelial Cell Spheroids*

By day 6 after beginning of the cocultures, the three-dimensional tumor cell–only spheroids (4T1) grew up to a diameter of approximately 200 μm, whereas the tumor-endothelial cell spheroids reached a size of approximately 400 μm in hanging drops of medium (Figure 1*A*). The tumor-endothelial cell spheroids grew to 800 μm when transferred to low-binding 96-well plates by day 12, remaining very round and viable even after 2 weeks (Figure 1*D*). Confocal microscopy using MitoTracker Red, a dye that stains the mitochondria red in living cells, was performed to establish these three-dimensional forms as spheroids. Whereas the 4T1 tumor cells were detected by the expression of the GFP, the mitochondrial staining of 2H11 endothelial cells made them fluoresce red in the overlay of red and green fluorescent images (Figure 1, *B* and *D*). The confocal images clearly indicated a physical interaction between tumor and endothelial cells. The tumor cell–only spheroids, which were almost half the size (Figure 1*B*), however, showed a tendency of disintegrating into clumps by day 8 onward and, when transferred to low-binding 96-well plates, started to adhere to the bottom and acquire a monolayer cell culture phenotype by day 10. H&E-stained sections of the spheroids in hanging drops at day 10 also confirmed a compact spheroid with small luminal structures formed in tumor-endothelial cell spheroids. On the contrary, H&E sections of spheroids prepared with tumor cells only revealed a loosely packed, disintegrating spheroidal form with large luminal structures (Figure 1*C*). Therefore, the 9- to 12-day window was used for treatment and for assessing the response of the spheroids to drugs and radiation *in vitro* studies. The spheroids were kept in the 96-well plates for not more than 48 hours for any of the *in vitro* studies.

Endothelial Cell Identification in Tumor-Endothelial Spheroids

We assessed the distribution of vWF, an endothelial cell marker and CD34, a protein that is expressed in tumor-endothelial cells by immunostaining of tumor-endothelial spheroid sections. Interestingly, the distribution of these proteins in the tumor-endothelial spheroids revealed that the endothelial cells, although introduced to the hanging drops of GFP-4T1 tumor cells at day 3, were able to penetrate into the core, initiating short tube-like formations (Figure 2*A*). Immunoblot analysis for galectin-1 and CD34 in lysates prepared from tumor cell–only and tumor-endothelial spheroids showed an

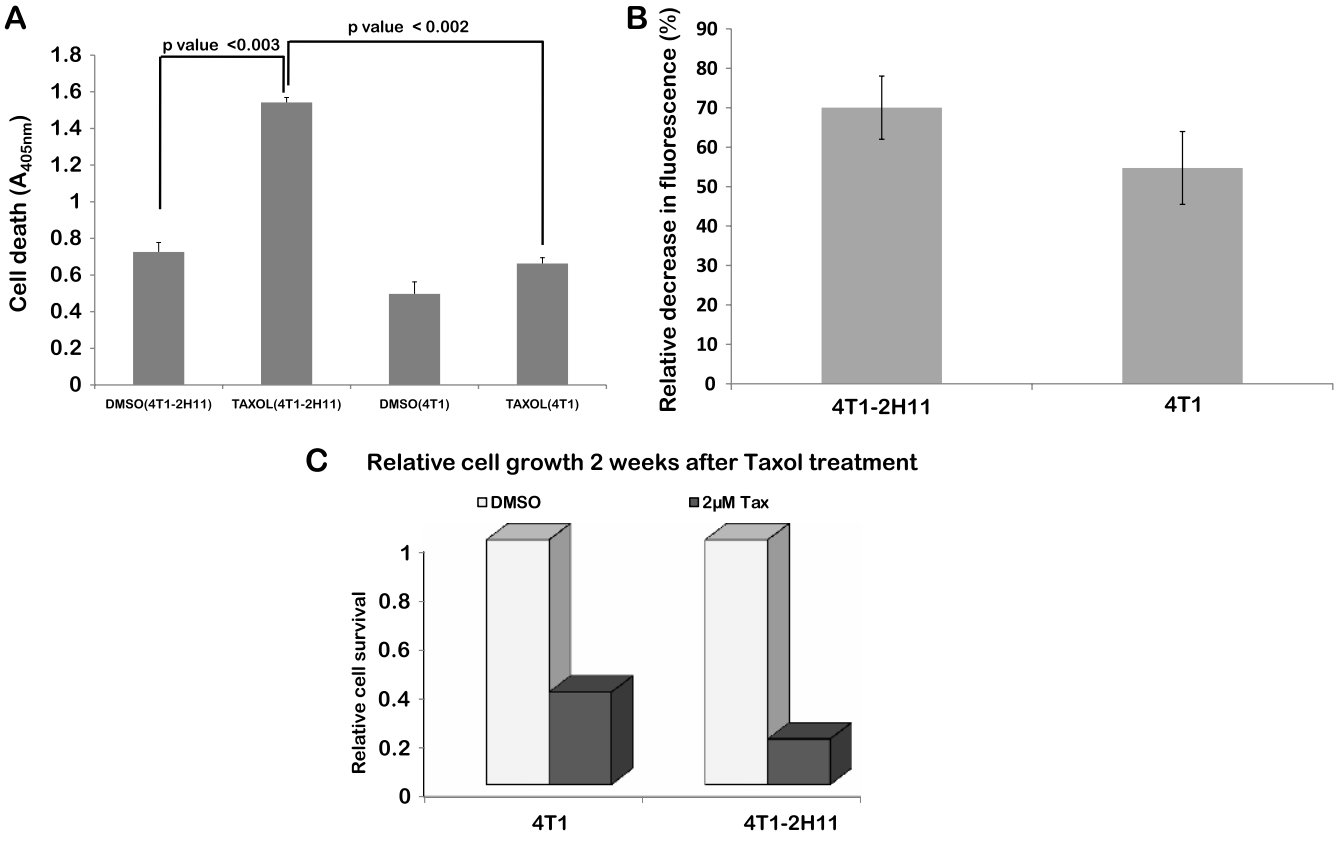

Figure 3. Presence of 2H11 murine endothelial cells in the three-dimensional spheroid cocultures with GFP-4T1 tumor cells sensitizes the Taxol-resistant GFP-4T1 cells to Taxol. (A) Relative cell death in control- and 2 μM Taxol–treated tumor cell–only or tumor-endothelial cell spheroids assessed at 48 hours using a cell death ELISA kit (Roche). (B) Relative decrease in fluorescence after Taxol treatment in the three-dimensional spheroids. (C) Relative cell survival 2 weeks after Taxol treatment.

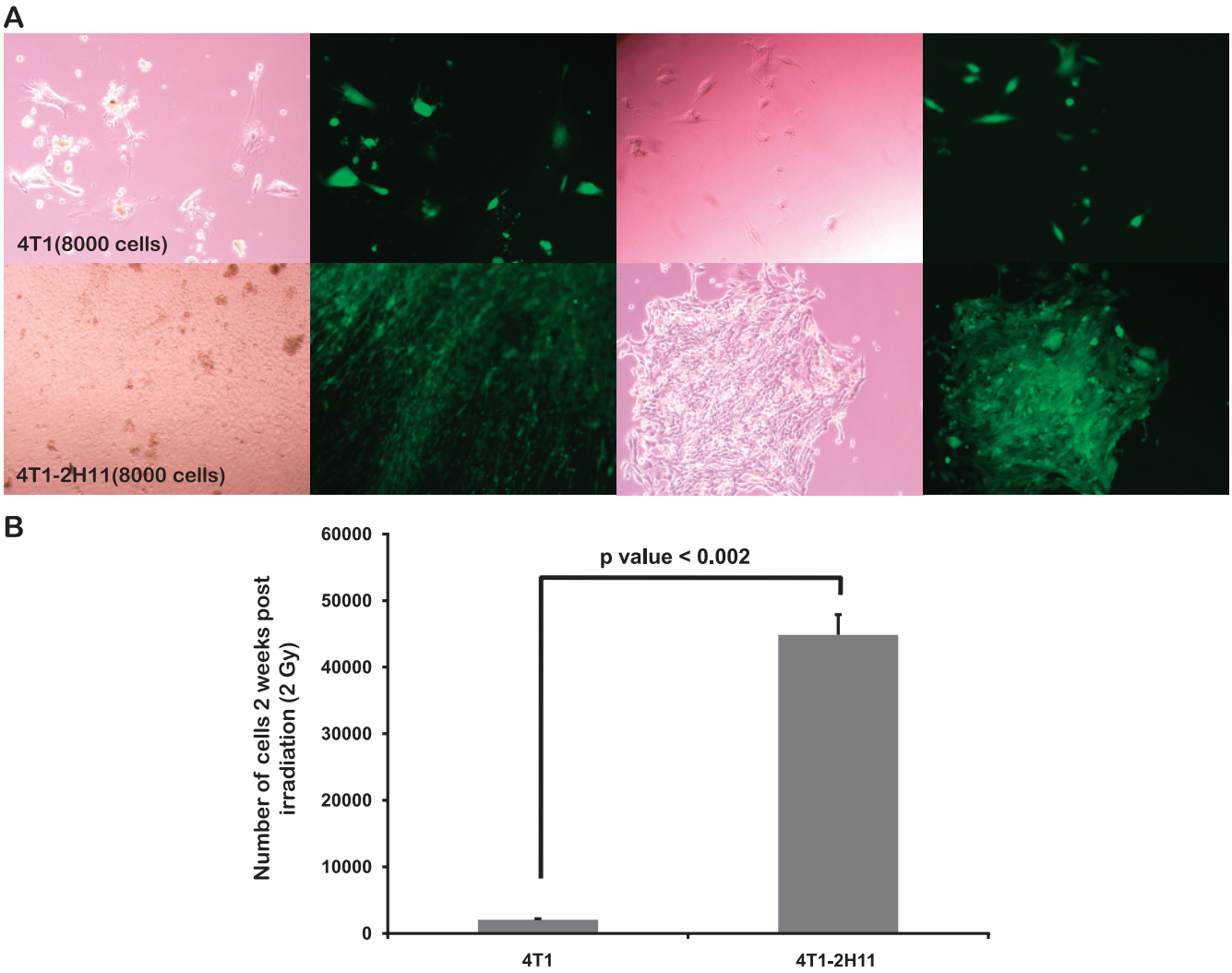

Figure 4. Presence of 2H11 endothelial cells in the three-dimensional spheroid cocultures with GFP-4T1 tumor cells protects the GFP-4T1 cells from radiation. (A) The tumor cell–only and tumor-endothelial three-dimensional spheroids were irradiated at 2 Gy; multiple spheroids of each type were pooled together, trypsinized, and plated as indicated onto a six-well culture dish. Phase-contrast and fluorescence images were taken 2 weeks after plating. (B) The graph depicts the final cell count after 2 weeks.

elevated expression of these tumor-endothelial cell–specific proteins in the tumor-endothelial spheroids (Figure 2*B*). Galectin-1 overexpression in recent reports has been shown to be associated with the tumor microenvironment, particularly in response to the tumor and endothelial cell interaction [20,21].

Response of Tumor and Tumor-Endothelial Spheroids to Taxol

The presence of murine 2H11 endothelial cells in three-dimensional spheroids generated from GFP-4T1 (a normally Taxol-resistant cell line) [11] made them more sensitive to Taxol treatment. We observed approximately 50% more cell death and 33% relative decrease in green fluorescence signal when normalized to treatment with DMSO in tumor-endothelial spheroids when compared to tumor cell–only spheroids (Figure 3, *A* and *B*) by 48 hours of exposure to 2 μM Taxol. Because these experiments were performed in extremely low-volume and high-drug concentration that was dissolved in DMSO, we have normalized all the results to DMSO-alone treatment. The cells from spheroids 48 hours after Taxol treatment were replated to assess survival after 2 weeks. The relative cell survival in the cells derived from the tumor-endothelial spheroids after treatment correlated with the previous results and was approximately 50% less than the tumor cell–only spheroids (Figure 3*C*).

Response of Tumor and Tumor-Endothelial Spheroids to Radiation

Exposure of tumor-endothelial spheroids after transfer to low-binding 96-well plates to 2 Gy of ionizing radiation caused a decreased amount of radiation-induced cell death in the tumor cells. With the intention to perform clonogenic assays, a suspension was prepared from tumor or tumor-endothelial spheroids after irradiation, and 8000 cells were plated/well. No distinct colonies were obtained at 2 weeks after culture. However, phase-contrast and fluorescence images (Figure 4*A*) and total cell count (Figure 4*B*) showed a significant increase in the number of GFP-4T1 tumor cells in cultures originating from tumor-endothelial spheroids after irradiation in comparison to those initiated from tumor cell–only spheroids.

Neoangiogenesis and Molecular Analysis of Angiogenic Factors in Tumors Originating from Tumor Cell–Only Versus *Tumor-Endothelial Cell Spheroids in Dorsal Skinfold Window Chamber Implants of Athymic Nude Mice*

Tumors initiating from transplanted tumor-endothelial cell spheroids implanted at day 10 after coculture showed rapid neovascularization within 14 days after implantation. Despite the fact that we had added double the number of tumor cells in the tumor cell–only spheroids, they showed little evidence of vascularization in this time frame (Figure 5*A*) and required approximately 26 days to get to the same level of neovascularization (data not shown). Blood vessel extraction using the vascular segmentation MATLAB code showed a distinct network of vessel in the tumor-endothelial cell spheroid implants. In the tumor cell–only spheroid implants, the vessels formed were in short discontinuous stretches (Figure 5*B*). Lysates from tumors excised from window chambers at 14 days after implantation were probed for the presence of 53 angiogenic factors using the customized Mouse Angiogenesis Antibody Array from R&D Systems. Many proangiogenic factors were upregulated in the tumors originating from tumor-endothelial cell spheroids in comparison to the tumors obtained from tumor cell–only spheroids (Figure 6*A*). Ingenuity pathway analysis revealed that several of them were functionally associated (Figure 6*B*). Four of

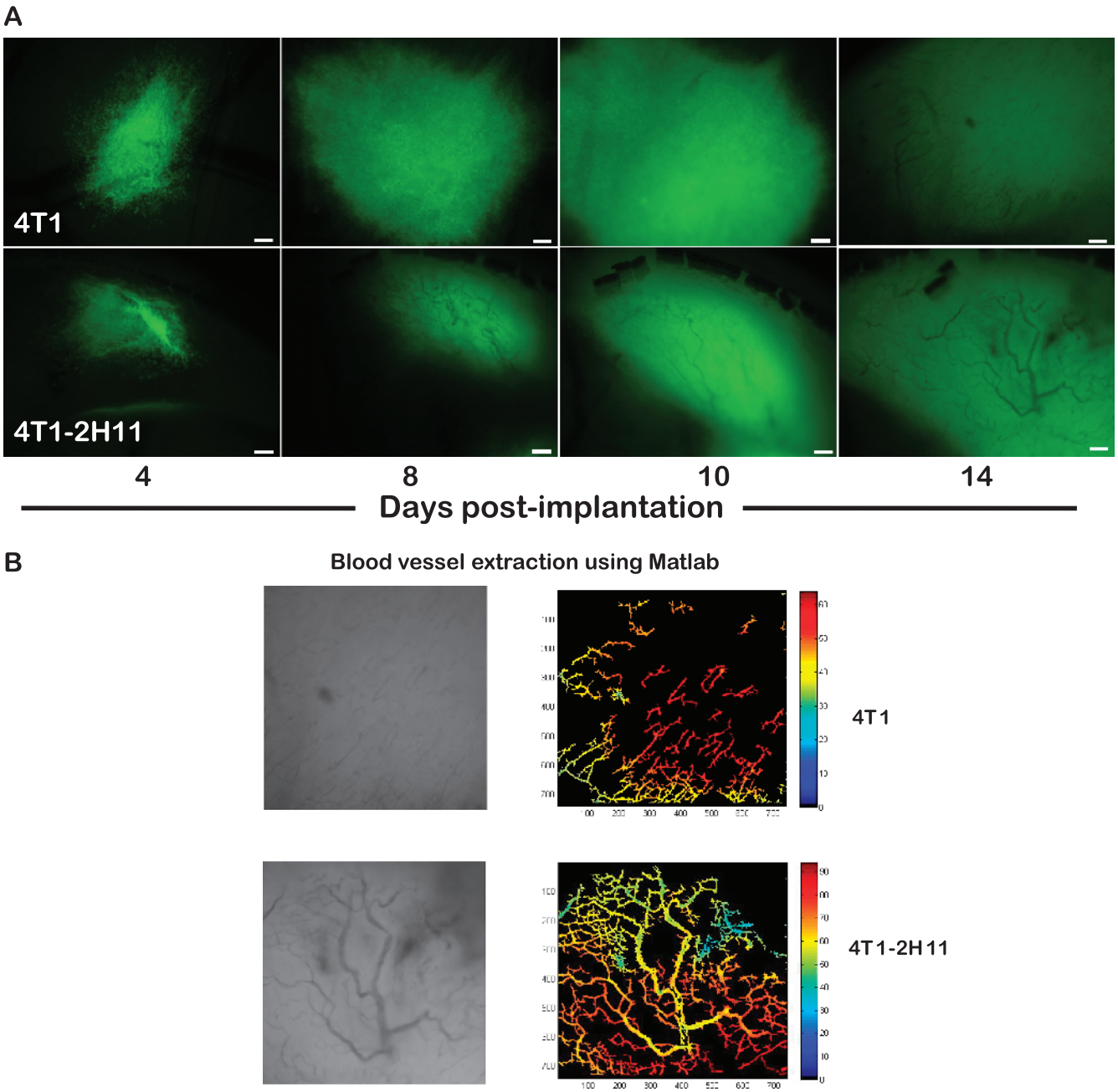

Figure 5. Profuse neovascularization in window chamber implanted with tumor-endothelial spheroid. (A) Images (4×) of window chambers implanted with tumor-endothelial spheroids showing profuse neovascularization by 14 days (lower panel) in comparison to 4T1 tumor spheroids alone (upper panel). Bar, 200 μm. (B) Vascular tree structure of blood vessels in the window chamber implants at day 14 after implantation. Left panel, Image in grayscale of the vascular structure. Right panel, Vascular tree structure was extracted using MATLAB-based vessel extraction technique, and the binary images extracted were assigned with an initial image intensity profile.

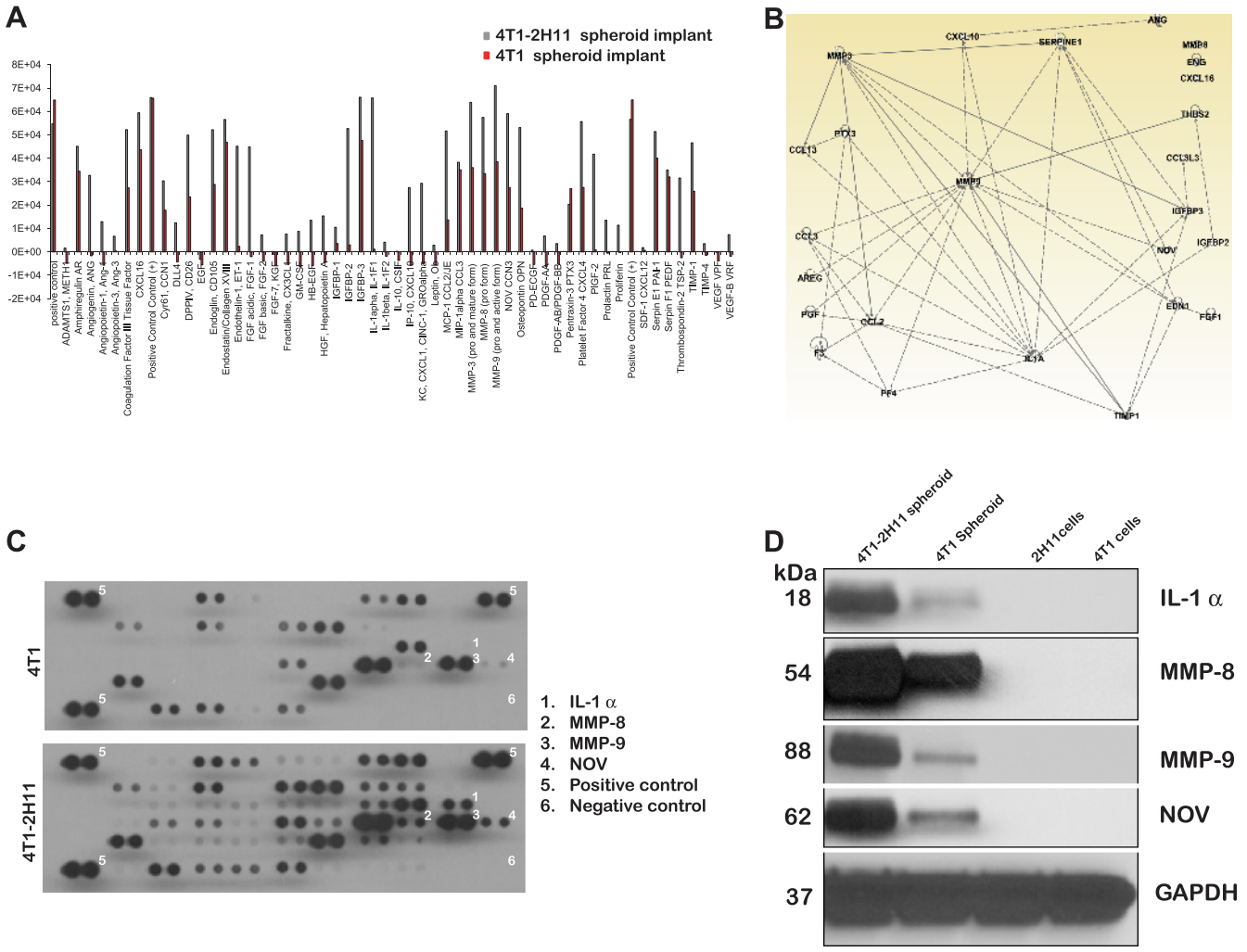

Figure 6. Pronounced up-regulation of angiogenic factors in tumor tissue derived from tumor-endothelial spheroid dorsal skinfold implant in nude mice. (A) Mouse angiogenesis antibody array: Quantification of pixel intensity as a measure of protein expression from lysates of tumor tissue derived from tumor cell–only and tumor-endothelial cell spheroids grown in window chamber of nude mice. (B) Ingenuity pathway analysis showing the interaction of some of the angiogenic proteins overexpressed in the tumor tissue derived from tumor-endothelial cell spheroids in comparison to the tumor cell–only spheroids. (C) Mouse angiogenesis antibody array blots probed with tumor lysates from GFP-4T1 and GFP-4T1–2H11 showing the expression of proteins that were selected for reverse-phase immunoblot analysis. (D) Validation by Western blot of four angiogenic factors distinctly upregulated in the lysates from tumor-endothelial spheroid–derived tissue and not in the 4T1 and 2H11 cells grown in monolayer cell cultures.

the significantly upregulated and functionally associated angiogenic proteins such as interleukin 1α, nephroblastoma overexpressed (NOV/CCN3), and members of the matrix metalloproteinase family (MMP-8 and -9) were then selected to be validated by Western immunoblot analysis. Interestingly, the expression of these four proteins while upregulated in the tumor lysates from tumor-endothelial cell spheroids compared with lysates of tumors from tumor cell–only spheroids was completely absent in whole-cell lysates of GFP-4T1 tumor or 2H11 endothelial cells growing in two-dimensional cultures (Figure 6, *C* and *D*).

Tumor Progression and Metastasis from Tumor Cell–Only Versus *Tumor-Endothelial Cell Spheroids Implanted in Rear Limb of Athymic Nude Mice*

Tumor cell implants in the rear limb have been used in many studies as an *in vivo* murine model to reliably measure tumor growth/volume by the caliper method [22–25] and are routinely performed in our laboratory [26,27]. When inoculated subcutaneously into the rear limb of mice, tumors originating from tumor-endothelial cell spheroids were palpable noticeably earlier than in tumors originating from the tumor cell–only spheroids. These spheroids were inoculated in duplicate at days 10 and 21 of coculture in hanging drops. Relative tumor growth in both sets of animals was greater in the tumors originating from 4T1-2H11 spheroids (Figure 7*A*). The mice inoculated with spheroids at days 10 and 21 in hanging drops were killed at days 33 and 45, respectively, after implantation. The metastasis was clearly more pronounced in mice when analyzed for GFP signal in lungs from tumor-endothelial spheroid implanted mice (Figure 7, *B* and *C*). Further, metastatic lesions were more numerous and larger in H&E-stained lung sections from mice bearing primary tumors originating from the tumor-endothelial cell spheroids (Figure 7*D*).

Discussion

Preclinical cell and animal models for cancer are typically used (i) to serve as an aid in the investigation of the basic biologic principles of

cancer, (ii) as an assay for the preclinical development of anticancer drugs or (iii) as a tool for discovering new clinical agents and assays. One of the most important concepts in preclinical modeling is "predictive utility" [28], and this is especially a critical need for the field of antiangiogenesis research where surrogate markers for activity and/or effect have been difficult to uncover. The culture of tumor cells within natural and synthetic extracellular matrix mimics and three-dimensional microenvironment conditions has been shown to clearly alter tumor cell signaling and has led to the development of more pathologically relevant cancer models [29–32]. However, the multiple variables typically inherent in the transition from two-dimensional to three-dimensional make it difficult to define the underlying mechanisms and importance of these changes. Therefore, to investigate the multicellular interactions involved in tumor growth and angiogenesis, we hypothesized that a multicellular scaffold-free aggregate formed as a consequence of gravity-enforced self-assembly in a self-contained microenvironment may be instructive. The use of gravity-enforced cell assembly has multiple potential benefits. It allows for precise size control preventing oxygen and nutrient limitations and is compatible with a variety of cell types; moreover, cell mobility during assembly enables natural intercellular organization. It also facilitates the development of an extracellular matrix, without interfering with cell regulatory networks. In addition, because it requires very low volumes, it is compatible with high-throughput assay systems. Although the *in vitro* model cannot account for all aspects of tumor grown *in vivo*, our studies clearly show that multicellular spheroids composed of both tumor and endothelial cells when grown as hanging drops have altered properties for treatment response *in vitro* and enhance tumor growth, angiogenesis, and progression when implanted *in vivo*. Nevertheless, the multicellular spheroid may allow more accurate modeling of the initial primary or micrometastatic stages of solid tumor progression than would be possible in a living

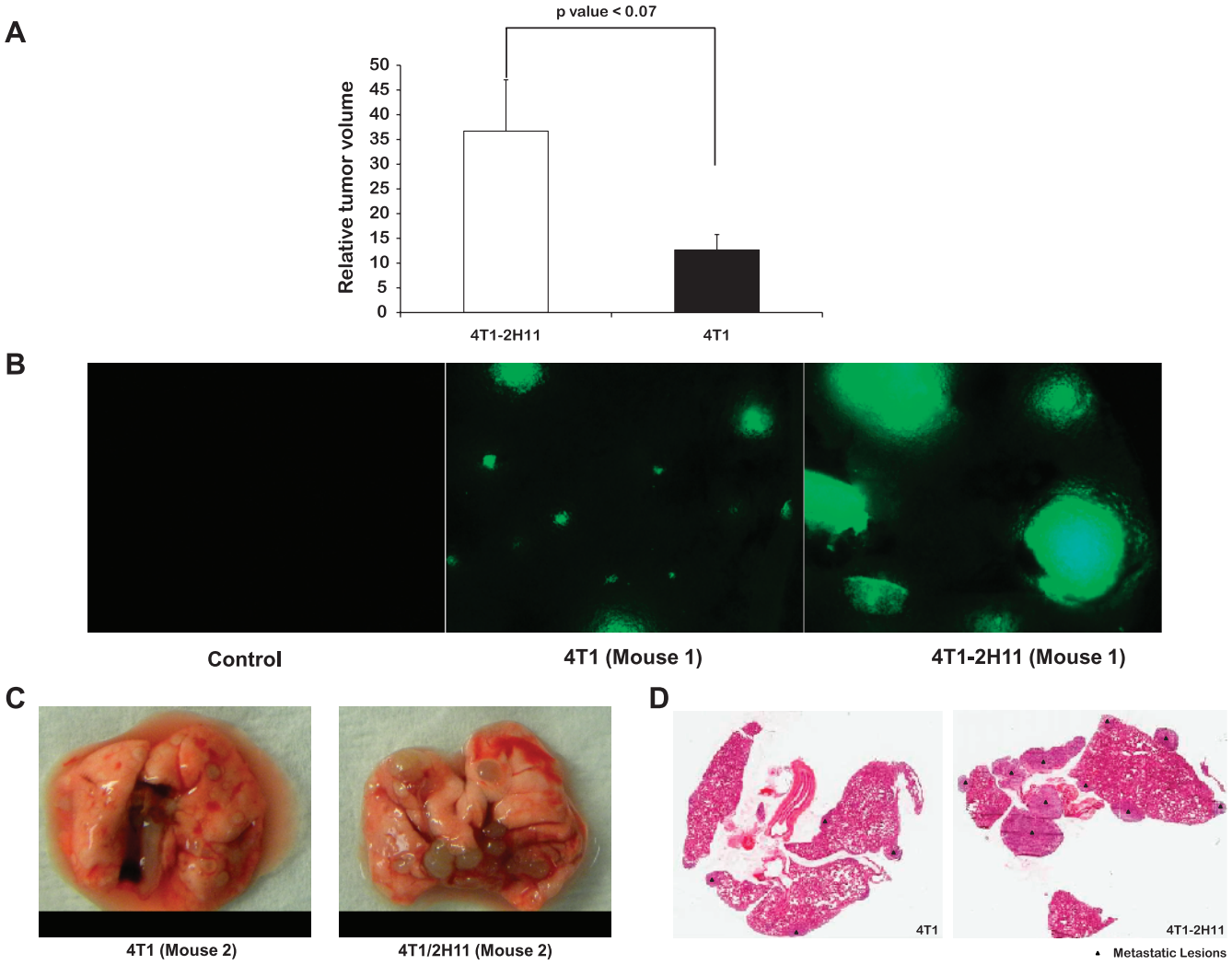

Figure 7. Increase in growth and aggressive metastasis to the lung of tumors originating from tumor-endothelial cell spheroids. (A) Tumors derived from tumor-endothelial cell spheroids implanted in rear limb of athymic nude mice exhibited enhanced growth rate in comparison to those derived from tumor cell–only spheroids. Values on the *y* axis represent the relative tumor volume (the ratio of tumor volume at day 33 to the tumor volume on the day palpable tumors were observed in the mice with 4T1 tumor spheroid implants). Results represent mean ± SD ($n = 3$). There is a significant difference ($P < .07$) in the relative tumor volume between the 4T1-2H11 and 4T1 measurements (three mice each) at $\alpha = 0.01$. Metastasis as observed by occurrence of diseased lungs with metastatic lesions was more aggressive in mice with primary tumors originating from tumor-endothelial cell spheroids. (B) Image of lung under fluorescence microscope at 4×. (C) Excised lungs at day 33 after implantation. (D) H&E-stained sections of lungs.

tissue. The molecular and cellular factors that drive these processes, and which treatment strategy best defeats them, are the ongoing focus of work in our group.

Cocultivation of tumor and endothelial cells causes reprogramming of the signaling in and between the two cell types, which results in a phenotypic switch that includes growth, migration, activation, and morphogenic changes like the formation of a network resembling the neovasculature. There have been several studies that have reported these changes to be associated with the coordinated changes of gene expression profiles from the tumor-endothelial interaction [33–36]. Coculture studies have also suggested various degrees of altered response of tumor cells to radiation, cytotoxic or antiangiogenic agents, and gene therapy [35,37–41]. The ability of these tumor-endothelial spheroids to enhance angiogenesis and metastasis *in vivo* further authenticates the importance of studying the crosstalk mechanisms between these cell types. Molecular and immunohistochemical studies are underway to characterize the "angiogenic switch" in the tumor-endothelial spheroids developed *in vitro*. We are also examining other murine and mammalian tumor and endothelial cell types to further establish this valuable preclinical model system. Our initial results indicate that this model may provide an excellent opportunity to comprehensively evaluate cancer therapeutics against an environment similar to occult cancer or micrometastases to generate more predictive preclinical data.

For example, using GFP-expressing 4T1 mouse mammary epithelial cells and murine 2H11 endothelial cells, we have shown that the presence of endothelial cells in the tumor microenvironment alters the response of the 4T1 tumor cells to both chemotherapy and radiation. Our studies reveal that the 4T1 tumor cells, normally resistant to Taxol at 2 μM [11], become sensitive to the same drug concentration when in coculture with the 2H11 endothelial cells (Figure 3). Conversely, the presence of endothelial cells in three-dimensional coculture with the tumor cells makes the tumor cells more resistant to 2 Gy of radiation (Figure 4). A better understanding of the tumor microenvironment may explain and predict why many therapies do not reach the expected level of activity in the patient.

Tumor spheroid implants in window chambers on the dorsal skinfold of rodents have been used routinely in translational studies [18,42–44]. Although some aspects of this model are artificial to true solid tumor growth, the window chamber model allows unmatched ability for longitudinal imaging of tumor growth and neovascularization in the living animal [45–47]. Using multiwavelength intravital imaging, we found rapid neovascularization in tumors originating from tumor-endothelial spheroid window chamber implants in comparison to tumors initiated from tumor spheroids only, again indicative of the functional significance of the presence of endothelial cells in the microenvironment (Figure 5). These distinct differences in tumor growth and vascularization were reflected in an antibody array based molecular analysis of tumor lysates showing up-regulation of proangiogenic factors in window chamber tumors originating from tumor-endothelial spheroids within a span of 14 days after implantation (Figure 6). Furthermore, our results in the window chamber were supported by another study where the growth of tumors in the rear limb of mice and metastasis to the lung originating from tumor-endothelial spheroids was much faster than in those from tumor spheroids alone (Figure 7, *A-D*). Thus, we conclude that the coculture of tumor and endothelial cells in the spheroids allows the process of tumor growth and angiogenesis to be enhanced/accelerated *in vivo* and that certain protein expression patterns, such as those we have identified, play a role in this enhanced growth. In 1941, Greene first showed the ability of avascular tumors to grow in the anterior chamber of the rabbit eye. These avascular tumors, however, continued to remain dormant and failed to grow when transplanted in the same way in guinea pigs [48,49]. The initial studies of tumor cell implants in hind limb of rats did result in large intramuscular tumors but no metastasis to the lung [50]. We noted the similarity between these studies done long ago showing the latency of avascular tumors to grow and metastasize *in vivo* and our *in vitro/in vivo* studies where inclusion of 2H11 endothelial cells in the GFP-4T1 tumor spheroids accelerated the process of tumor growth and metastasis.

In summary, the hanging drop tumor-endothelial cell strategy *in vitro* and subsequent transplant to the window chamber or rear limb *in vivo* is a newly created preclinical model system to better understand mechanisms governing tumor initiation, growth, angiogenesis, and progression. In addition, the response of these systems to experimental or established therapeutics will allow important observations about the cellular, molecular, and physiological aspects of tumor response. In addition, the importance of yet undefined modes of intercellular communication and support between tumor and endothelial cells may be uncovered to lead to new targets for cancer control. Efforts in our group are directed toward developing and improving strategies for tumor-specific radiation therapy and/or drug delivery, by identifying surrogate markers of tumor progression, before and after treatment.

Acknowledgments

The authors thank Peter Corry for his constructive suggestions during the course of the study and Jerry Ware for providing us the von Willebrand factor antibody.

References

[1] Hanahan D and Weinberg RA (2000). The hallmarks of cancer. *Cell* **100**, 57–70.
[2] Fritz P, Weber KJ, Frank C, and Flentje M (1996). Differential effects of dose rate and superfractionation on survival and cell cycle of v79 cells from spheroid and monolayer culture. *Radiother Oncol* **39**, 73–79.
[3] Kobayashi H, Man S, Graham CH, Kapitain SJ, Teicher BA, and Kerbel RS (1993). Acquired multicellular-mediated resistance to alkylating agents in cancer. *Proc Natl Acad Sci USA* **90**, 3294–3298.
[4] Feder-Mengus C, Ghosh S, Weber WP, Wyler S, Zajac P, Terracciano L, Oertli D, Heberer M, Martin I, Spagnoli GC, et al. (2007). Multiple mechanisms underlie defective recognition of melanoma cells cultured in three-dimensional architectures by antigen-specific cytotoxic T lymphocytes. *Br J Cancer* **96**, 1072–1082.
[5] Gaya A, Daley F, Taylor NJ, Tozer G, Qureshi U, Padhani A, Pedley RB, Begent R, Wellsted D, Stirling JJ, et al. (2008). Relationship between human tumour angiogenic profile and combretastatin-induced vascular shutdown: an exploratory study. *Br J Cancer* **99**, 321–326.
[6] Hasina R, Whipple ME, Martin LE, Kuo WP, Ohno-Machado L, and Lingen MW (2008). Angiogenic heterogeneity in head and neck squamous cell carcinoma: biological and therapeutic implications. *Lab Invest* **88**, 342–353.
[7] van Kempen LC and Leenders WP (2006). Tumours can adapt to anti-angiogenic therapy depending on the stromal context: lessons from endothelial cell biology. *Eur J Cell Biol* **85**, 61–68.
[8] Zakarija A and Soff G (2005). Update on angiogenesis inhibitors. *Curr Opin Oncol* **17**, 578–583.
[9] Timmins NE, Dietmair S, and Nielsen LK (2004). Hanging-drop multicellular spheroids as a model of tumour angiogenesis. *Angiogenesis* **7**, 97–103.
[10] Bausero MA, Bharti A, Page DT, Perez KD, Eng JW, Ordonez SL, Asea EE, Jantschitsch C, Kindas-Muegge I, Ciocca D, et al. (2006). Silencing the *hsp25* gene eliminates migration capability of the highly metastatic murine 4t1 breast adenocarcinoma cell. *Tumour Biol* **27**, 17–26.
[11] Luo T, Wang J, Yin Y, Hua H, Jing J, Sun X, Li M, Zhang Y, and Jiang Y (2010). (–)-Epigallocatechin gallate sensitizes breast cancer cells to paclitaxel in a murine model of breast carcinoma. *Breast Cancer Res* **12**, R8.

[12] Walter-Yohrling J, Morgenbesser S, Rouleau C, Bagley R, Callahan M, Weber W, and Teicher BA (2004). Murine endothelial cell lines as models of tumor endothelial cells. *Clin Cancer Res* **10**, 2179–2189.

[13] O'Connell KA and Rudmann AA (1993). Cloned spindle and epithelioid cells from murine Kaposi's sarcoma–like tumors are of endothelial origin. *J Invest Dermatol* **100**, 742–745.

[14] O'Connell KA and Edidin M (1990). A mouse lymphoid endothelial cell line immortalized by simian virus 40 binds lymphocytes and retains functional characteristics of normal endothelial cells. *J Immunol* **144**, 521–525.

[15] O'Connell K, Landman G, Farmer E, and Edidin M (1991). Endothelial cells transformed by SV40 T antigen cause Kaposi's sarcomalike tumors in nude mice. *Am J Pathol* **139**, 743–749.

[16] Kelm JM, Timmins NE, Brown CJ, Fussenegger M, and Nielsen LK (2003). Method for generation of homogeneous multicellular tumor spheroids applicable to a wide variety of cell types. *Biotechnol Bioeng* **83**, 173–180.

[17] Frost GI and Borgstrom P (2003). Real time *in vivo* quantitation of tumor angiogenesis. *Methods Mol Med* **85**, 65–78.

[18] Lehr HA, Leunig M, Menger MD, Nolte D, and Messmer K (1993). Dorsal skinfold chamber technique for intravital microscopy in nude mice. *Am J Pathol* **143**, 1055–1062.

[19] Gaustad JV, Brurberg KG, Simonsen TG, Mollatt CS, and Rofstad EK (2008). Tumor vascularity assessed by magnetic resonance imaging and intravital microscopy imaging. *Neoplasia* **10**, 354–362.

[20] Thijssen VL, Barkan B, Shoji H, Aries IM, Mathieu V, Deltour L, Hackeng TM, Kiss R, Kloog Y, Poirier F, et al. (2010). Tumor cells secrete galectin-1 to enhance endothelial cell activity. *Cancer Res* **70**, 6216–6224.

[21] Thijssen VL, Postel R, Brandwijk RJ, Dings RP, Nesmelova I, Satijn S, Verhofstad N, Nakabeppu Y, Baum LG, Bakkers J, et al. (2006). Galectin-1 is essential in tumor angiogenesis and is a target for antiangiogenesis therapy. *Proc Natl Acad Sci USA* **103**, 15975–15980.

[22] Hallahan D, Geng L, Qu S, Scarfone C, Giorgio T, Donnelly E, Gao X, and Clanton J (2003). Integrin-mediated targeting of drug delivery to irradiated tumor blood vessels. *Cancer Cell* **3**, 63–74.

[23] Nechushtan H, Pham D, Zhang Y, Morgensztern D, Yi KH, Shin SU, Federoff HJ, Bowers WJ, Tolba KA, and Rosenblatt JD (2008). Augmentation of anti-tumor responses of adoptively transferred $CD8^+$ T cells in the lymphopenic setting by HSV amplicon transduction. *Cancer Immunol Immunother* **57**, 663–675.

[24] Linkous A, Geng L, Lyshchik A, Hallahan DE, and Yazlovitskaya EM (2009). Cytosolic phospholipase A_2: targeting cancer through the tumor vasculature. *Clin Cancer Res* **15**, 1635–1644.

[25] Henshaw J, Mossop B, and Yuan F (2011). Enhancement of electric field–mediated gene delivery through pretreatment of tumors with a hyperosmotic mannitol solution. *Cancer Gene Ther* **18**, 26–33.

[26] Griffin RJ, Williams BW, Wild R, Cherrington JM, Park H, and Song CW (2002). Simultaneous inhibition of the receptor kinase activity of vascular endothelial, fibroblast, and platelet-derived growth factors suppresses tumor growth and enhances tumor radiation response. *Cancer Res* **62**, 1702–1706.

[27] Griffin RJ, Williams BW, Bischof JC, Olin M, Johnson GL, and Lee BW (2007). Use of a fluorescently labeled poly-caspase inhibitor for *in vivo* detection of apoptosis related to vascular-targeting agent arsenic trioxide for cancer therapy. *Technol Cancer Res Treat* **6**, 651–654.

[28] Olive KP and Tuveson DA (2006). The use of targeted mouse models for preclinical testing of novel cancer therapeutics. *Clin Cancer Res* **12**, 5277–5287.

[29] Brantley-Sieders DM, Dunaway CM, Rao M, Short S, Hwang Y, Gao Y, Li D, Jiang A, Shyr Y, Wu JY, et al. (2011). Angiocrine factors modulate tumor proliferation and motility through EphA2 repression of Slit2 tumor suppressor function in endothelium. *Cancer Res* **71**, 976–987.

[30] Chung S, Sudo R, Mack PJ, Wan CR, Vickerman V, and Kamm RD (2009). Cell migration into scaffolds under co-culture conditions in a microfluidic platform. *Lab Chip* **9**, 269–275.

[31] Fischbach C, Chen R, Matsumoto T, Schmelzle T, Brugge JS, Polverini PJ, and Mooney DJ (2007). Engineering tumors with 3D scaffolds. *Nat Methods* **4**, 855–860.

[32] Wang F, Weaver VM, Petersen OW, Larabell CA, Dedhar S, Briand P, Lupu R, and Bissell MJ (1998). Reciprocal interactions between β_1-integrin and epidermal growth factor receptor in three-dimensional basement membrane breast cultures: a different perspective in epithelial biology. *Proc Natl Acad Sci USA* **95**, 14821–14826.

[33] Chen A, Cuevas I, Kenny PA, Miyake H, Mace K, Ghajar C, Boudreau A, Bissell MJ, and Boudreau N (2009). Endothelial cell migration and vascular endothelial growth factor expression are the result of loss of breast tissue polarity. *Cancer Res* **69**, 6721–6729.

[34] Buess M, Rajski M, Vogel-Durrer BM, Herrmann R, and Rochlitz C (2009). Tumor-endothelial interaction links the CD44(+)/CD24(–) phenotype with poor prognosis in early-stage breast cancer. *Neoplasia* **11**, 987–1002.

[35] Khodarev NN, Labay E, Darga T, Yu J, Mauceri H, Gupta N, Kataoka Y, and Weichselbaum RR (2004). Endothelial cells co-cultured with wild-type and dominant/negative p53-transfected glioblastoma cells exhibit differential sensitivity to radiation-induced apoptosis. *Int J Cancer* **109**, 214–219.

[36] Khodarev NN, Yu J, Labay E, Darga T, Brown CK, Mauceri HJ, Yassari R, Gupta N, and Weichselbaum RR (2003). Tumour-endothelium interactions in co-culture: coordinated changes of gene expression profiles and phenotypic properties of endothelial cells. *J Cell Sci* **116**, 1013–1022.

[37] Wang L, Shi WY, Yang F, Tang W, Gapihan G, Varna M, Shen ZX, Chen SJ, Leboeuf C, Janin A, et al. (2011). Bevacizumab potentiates chemotherapeutic effect on T-leukemia/lymphoma cells by direct action on tumor endothelial cells. *Haematologica* **96**, 927–931.

[38] Shi Q, Nguyen AT, Angell Y, Deng D, Na CR, Burgess K, Roberts DD, Brunicardi FC, and Templeton NS (2010). A combinatorial approach for targeted delivery using small molecules and reversible masking to bypass nonspecific uptake *in vivo*. *Gene Ther* **17**, 1085–1097.

[39] Paduch R, Kandefer-Szerszen M, and Piersiak T (2010). The importance of release of proinflammatory cytokines, ROS, and NO in different stages of colon carcinoma growth and metastasis after treatment with cytotoxic drugs. *Oncol Res* **18**, 419–436.

[40] Trepel M, Stoneham CA, Eleftherohorinou H, Mazarakis ND, Pasqualini R, Arap W, and Hajitou A (2009). A heterotypic bystander effect for tumor cell killing after adeno-associated virus/phage–mediated, vascular-targeted suicide gene transfer. *Mol Cancer Ther* **8**, 2383–2391.

[41] Sengupta S, Kiziltepe T, and Sasisekharan R (2004). A dual-color fluorescence imaging–based system for the dissection of antiangiogenic and chemotherapeutic activity of molecules. *FASEB J* **18**, 1565–1567.

[42] Brown E, Munn LL, Fukumura D, and Jain RK (2010). *In vivo* imaging of tumors. *Cold Spring Harb Protoc*. pdb.prot5452. DOI: 10.1101/pdb.prot5452.

[43] Moeller BJ, Cao Y, Li CY, and Dewhirst MW (2004). Radiation activates HIF-1 to regulate vascular radiosensitivity in tumors: role of reoxygenation, free radicals, and stress granules. *Cancer Cell* **5**, 429–441.

[44] Sckell A and Leunig M (2001). Dorsal skinfold chamber preparation in mice: studying angiogenesis by intravital microscopy. *Methods Mol Med* **46**, 95–105.

[45] Wang Y, Chen Q, and Yuan F (2005). Alginate encapsulation is a highly reproducible method for tumor cell implantation in dorsal skinfold chambers. *Biotechniques* **39**, 834, 836, 838–839.

[46] Tang Y, Borgstrom P, Maynard J, Koziol J, Hu Z, Garen A, and Deisseroth A (2007). Mapping of angiogenic markers for targeting of vectors to tumor vascular endothelial cells. *Cancer Gene Ther* **14**, 346–353.

[47] Bingle L, Lewis CE, Corke KP, Reed MW, and Brown NJ (2006). Macrophages promote angiogenesis in human breast tumour spheroids *in vivo*. *Br J Cancer* **94**, 101–107.

[48] Greene HS (1941). Heterologous transplantation of mammalian tumors: II. The transfer of human tumors to alien species. *J Exp Med* **73**, 475–486.

[49] Greene HS (1941). Heterologous transplantation of mammalian tumors: I. The transfer of rabbit tumors to alien species. *J Exp Med* **73**, 461–474.

[50] Stein-Werblowsky R (1978). On the latency of tumour cells. *Br J Exp Pathol* **59**, 386–389.

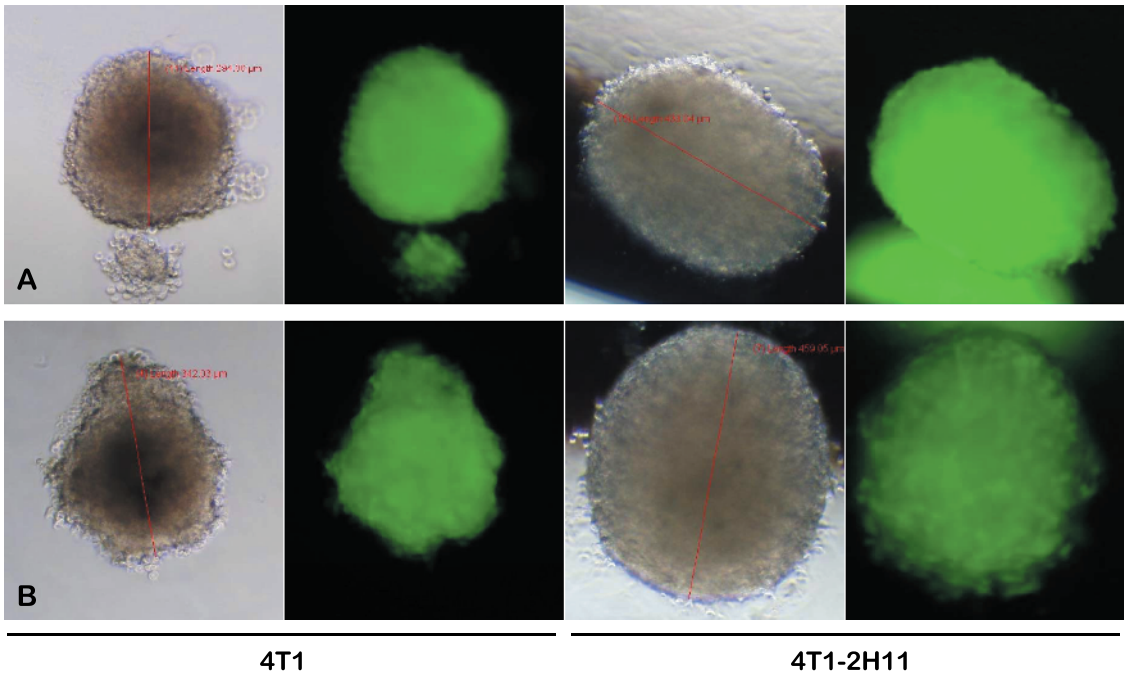

Figure W1. Spheroids at day 6 after addition of 200 (A) and 2000 (B) 4T1 tumor or 2H11 endothelial cells to the existing 4T1 hanging drop culture.